Gamma-rays, EUV Wave (Shock), and SEPs Associated with the M1.5 Behind-the-limb Flare on 2013-Oct-11

Melissa Pesce-Rollins
INFN–Pisa
melissa.pesce.rollins@pi.infn.it

on behalf of the Fermi-LAT collaboration
LWS-14 Nov 6, 2014

To be submitted to ApJ Letters:

Melissa Pesce-Rollins (INFN-Pisa, Italy),
Nicola Omodei, Vahe' Petrosian, **Wei Liu**, Fatima Rubio Da Costa, Qingrong Chen (Stanford Univ.)

Outline

1. Fermi solar flare detection overview

2. The first behind-the-limb > 100 MeV flare: 2013-Oct-11 M1.5

   2.1) Multiwavelength context
   2.2) Fermi gamma rays observations

3. Summary & Discussion

The *Fermi* Space Telescope

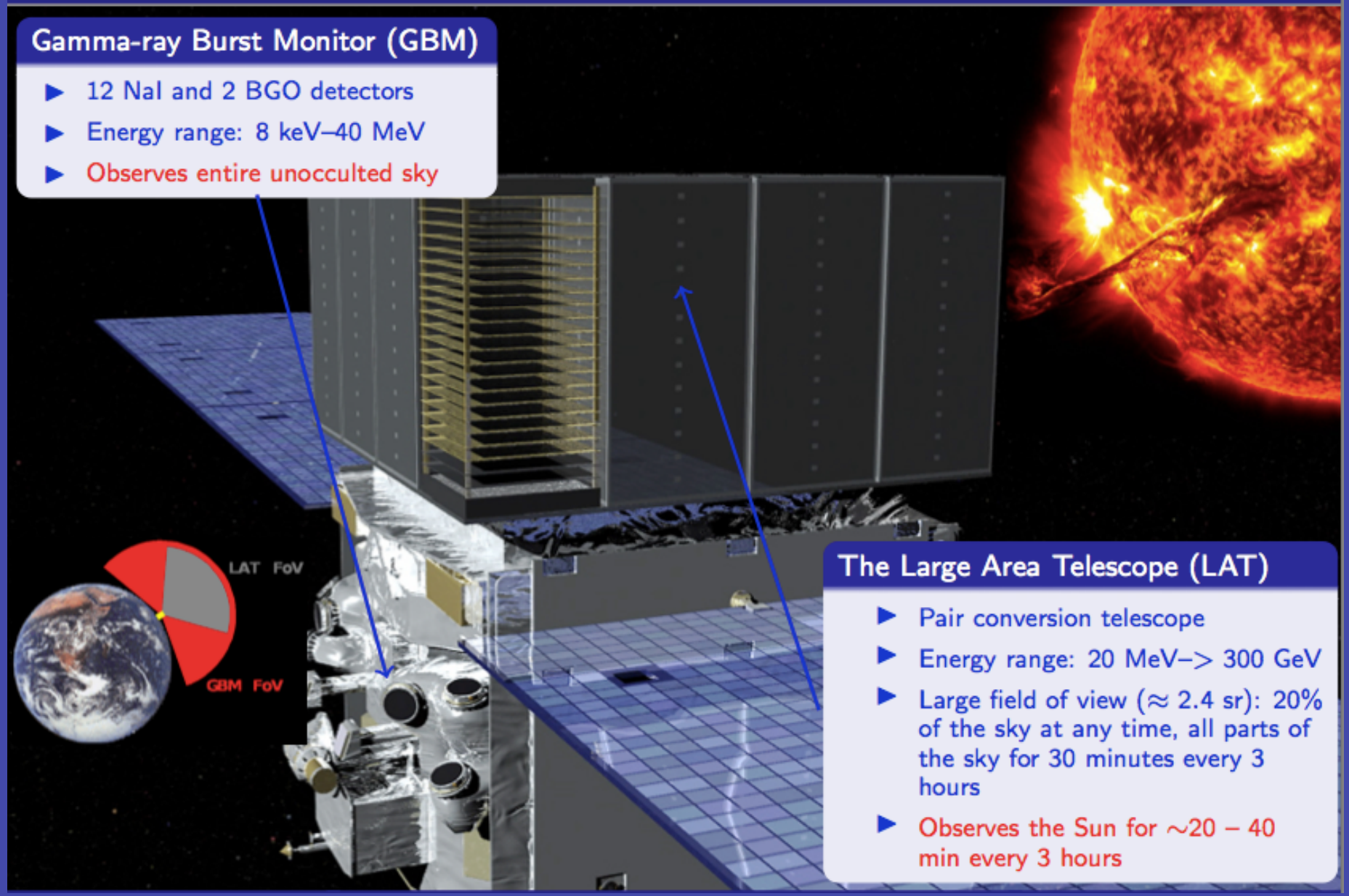

Gamma-ray Burst Monitor (GBM)

- 12 NaI and 2 BGO detectors
- Energy range: 8 keV–40 MeV
- Observes entire unocculted sky

The Large Area Telescope (LAT)

- Pair conversion telescope
- Energy range: 20 MeV–> 300 GeV
- Large field of view ($\approx$ 2.4 sr): 20% of the sky at any time, all parts of the sky for 30 minutes every 3 hours
- Observes the Sun for $\sim$20 – 40 min every 3 hours

1. Fermi solar flare detection

19 flares in 4 years (also see Gerry Share 2014 SPD/Boston talk)

Surprises:

1) γ-rays from not only X-class flares, but also M- and even C-flares – Fermi's superior sensitivity

2) Long duration (~20 hr) γ-rays

The Astrophysical Journal, 787:15 (13pp), 2014 May 20 Ackermann et al.

Table 1
Solar Flares Detected by the *Fermi* LAT from 2008 August to 2012 August

Date	*GOES* X-Ray Class, Start–End[d]	Type	Duration (hr)	CME Speed[a] (km s^{-1})	*Fermi* Time Window Start[d], Duration (minutes)	TS[b]	Flux[c]	Energy Flux[c]
2010 Jun 12	M2.0, 00:30-01:02	I	...	486	00:55, 0.8	LLE[e]	...	...
2011 Mar 7	M3.7, 19:43-20:58	I/S	10.7	2125	20:15, 25	230	1.9 ± 0.3	6.7 ± 1.0
		S			23:26, 36	520	3.5 ± 0.3	11.9 ± 1.1
2011 Mar 8		S			02:38, 35	450	3.5 ± 0.3	11.6 ± 1.1
					05:49, 35	200	1.9 ± 0.3	5.4 ± 0.7
2011 Jun 2	C2.7,9:42-9:50	I/S	0.8	976	09:43, 45	35	0.4 ± 0.2	1.4 ± 0.5
2011 Jun 7	M2.5, 06:16-06:59	S	2.2	1255	07:34, 53	570	3.6 ± 0.3	11 ± 0.9
2011 Aug 4	M9.3, 03:41-04:04	S	1.9	1315	04:59, 34	390	2.5 ± 0.3	7.9 ± 0.8
2011 Aug 9	X6.9, 07:48-08:08	I	...	1610	08:01, 3.3	LLE[e]	...	...
2011 Sep 6	X2.1, 22:12-22:24	I	0.6	575	22:17, 0.2	LLE[e]	...	...
		I/S			22:13, 35	[f]	[f]	
2011 Sep 7	X1.8, 22:32-22:44	S	2.1	792	23:36, 63	350	1.0 ± 0.1	3.5 ± 0.4
2011 Sep 24	X1.9, 09:21-09:48	I	...	1936	09:34, 0.8	LLE[e]	...	...
2012 Jan 23	M8.7, 03:38-04:34	I/S	5.7	1953	04:07, 51	180	0.8 ± 0.1	2.7 ± 0.4
		S			05:25, 69	650	2.1 ± 0.2	6.6 ± 0.5
		S			07:26, 16	69	3.7 ± 0.9	9.6 ± 2.2
		S			08:47, 35	97	2.6 ± 0.5	7.0 ± 1.3
2012 Jan 27	X1.7, 17:37-18:56	D	4.0	1930	19:45, 11	78	3.2 ± 0.8	9.6 ± 2.2
		S			21:13, 24	47	1.0 ± 0.3	2.8 ± 0.8
2012 Mar 5	X1.1, 02:30-04:43	I/S	5.3	1602	04:12, 49	69	0.5 ± 0.1	1.5 ± 0.3
		S			05:26, 71	250	0.9 ± 0.1	2.5 ± 0.3
		S			07:23, 28	39	0.8 ± 0.2	2.4 ± 0.7
2012 Mar 7	X5.4, 00:02-00:40	S	20.2	2684	00:46, 31	22000	[f]	[f]
	X1.3, 01:05–01:23	I/S		1785	00:46, 60	LLE[e]	...	...
					03:56, 32	16000	113.1 ± 2.0	400.5 ± 6.6
					07:07, 32	8900	71.9 ± 1.6	232.6 ± 4.9
					10:18, 32	1900	30.1 ± 1.5	91.9 ± 4.3
					13:29, 32	120	8.9 ± 1.9	29.9 ± 5.9
					19:51, 25	50	0.4 ± 0.1	1.7 ± 0.5
2012 Mar 9	M6.3, 03:22-04:18	D	5.7	844	05:17, 34	51	0.6 ± 0.2	2.0 ± 0.5
		S			06:52, 35	100	0.9 ± 0.2	2.8 ± 0.6
		S			08:28, 34	159	1.4 ± 0.2	4.3 ± 0.7
2012 Mar 10	M8.4, 17:15-18:30	D	4.3	1379	21:05, 30	43	0.4 ± 0.1	1.0 ± 0.3
2012 May 17	M5.1, 01:25-02:14	I/S	1.2	1582	02:18, 22	45	1.0 ± 0.3	3.4 ± 0.9
2012 Jun 3	M3.3, 17:48-17:57	I	0.2	605	17:52, 0.6	LLE[e]	...	...
		I/S			17:40, 23	300	3.2 ± 0.4	10.6 ± 1.2
2012 Jul 6	X1.1,23:15-23:49	I/S	0.9	892	23:19, 52	930	3.5 ± 0.2	10.4 ± 0.7

Ackmann et al. (2014 ApJ)

Long-duration (~20 hr) γ-rays detected by *Fermi*, way after flare impulsive phases, no more hard X-rays counterparts.

Particle accelerated by CME shocks travel back to the Sun to produce γ-rays?

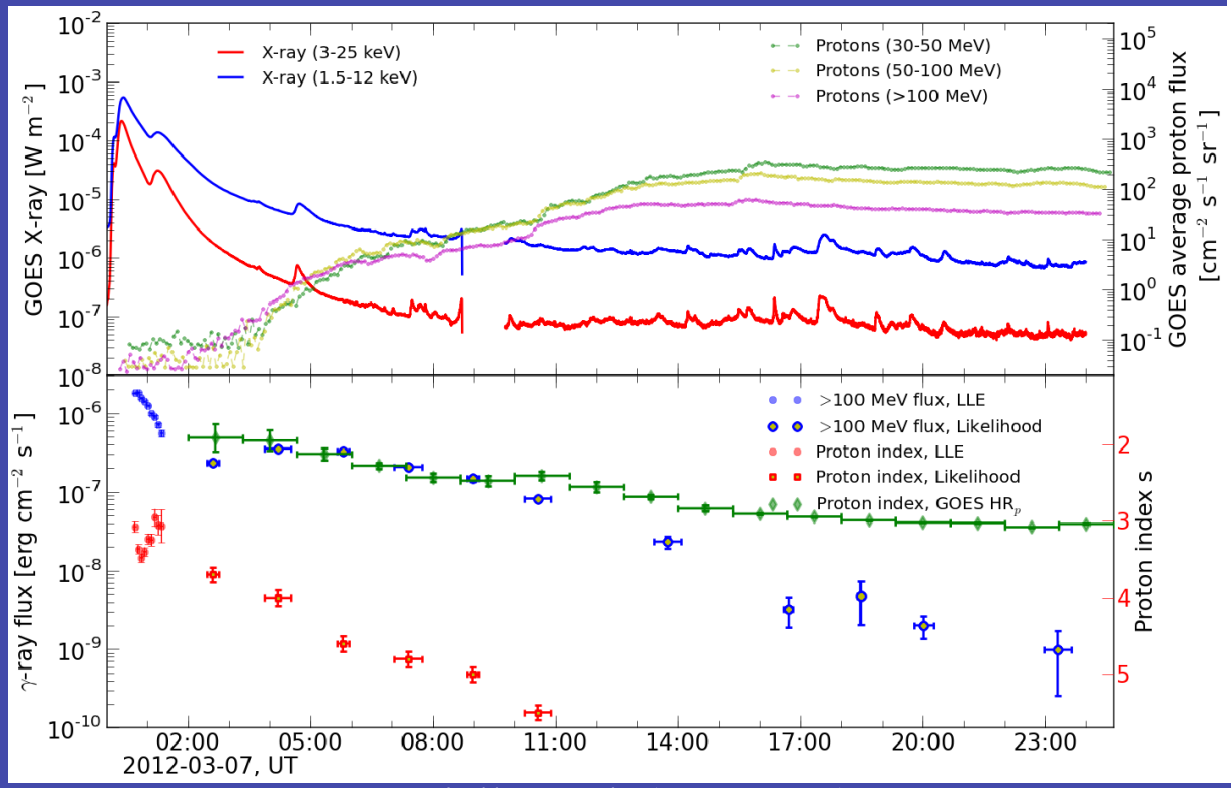

Ajello et al. (2014 ApJ)

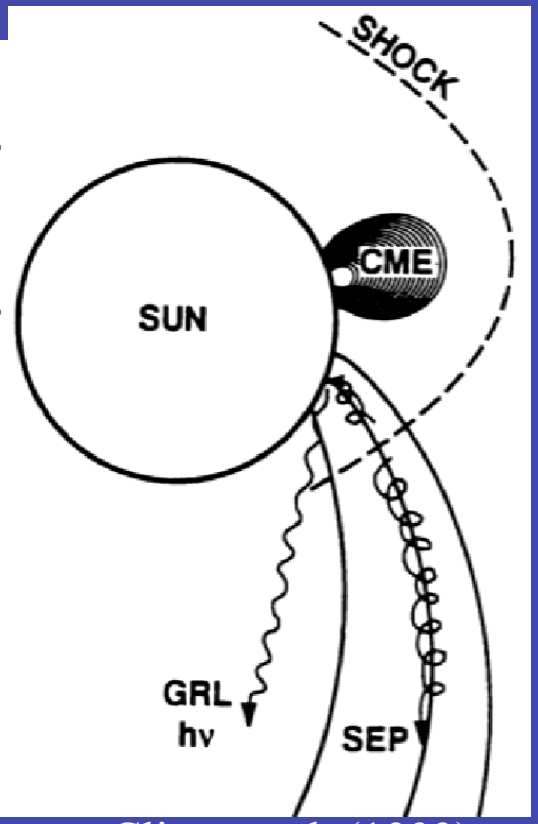

Cliver et al. (1993)

2. 2013-Oct-11 M1.5 flare, Fast (1200 km/s) CME seen by SOHO/LASCO

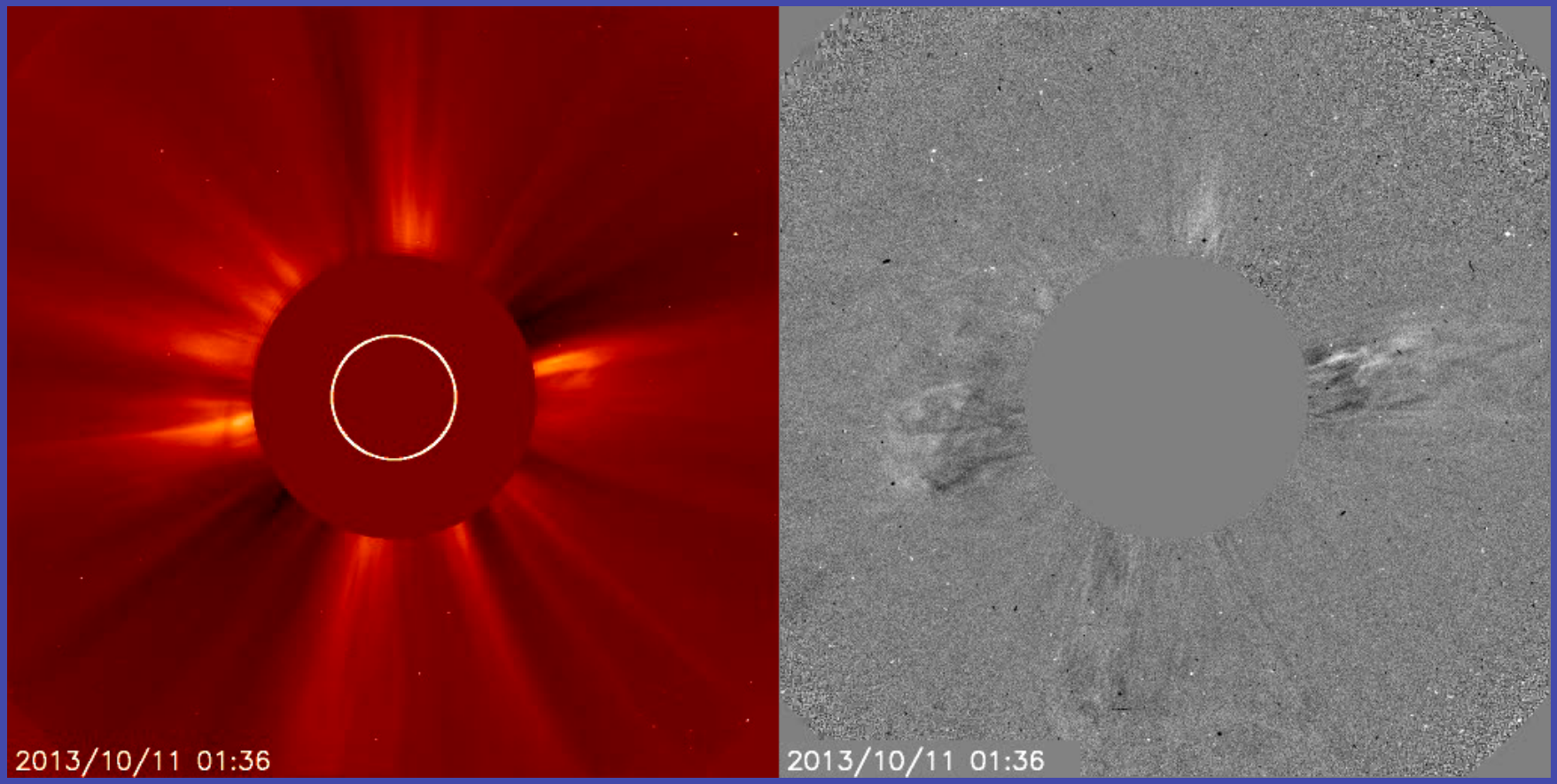

Light curves

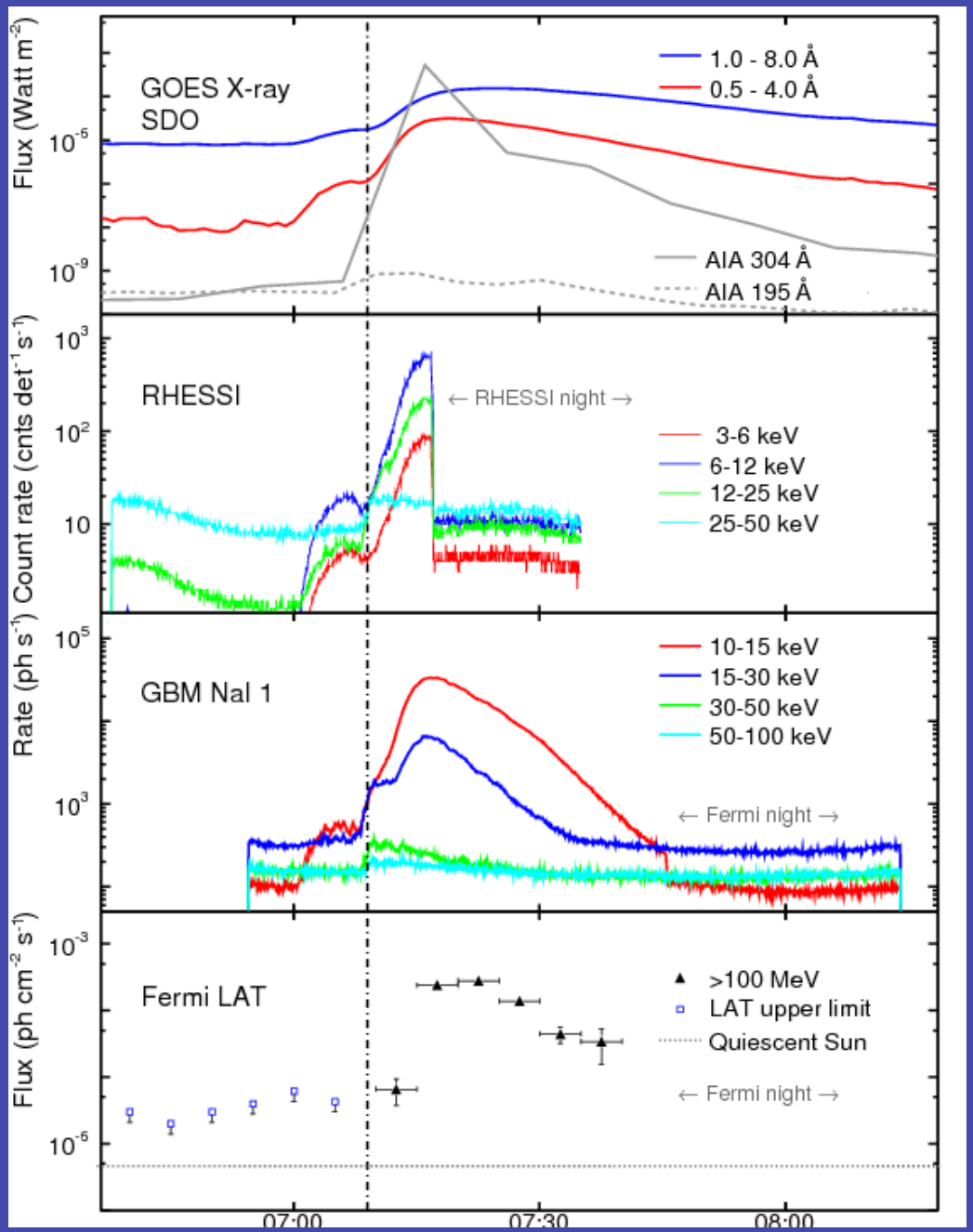

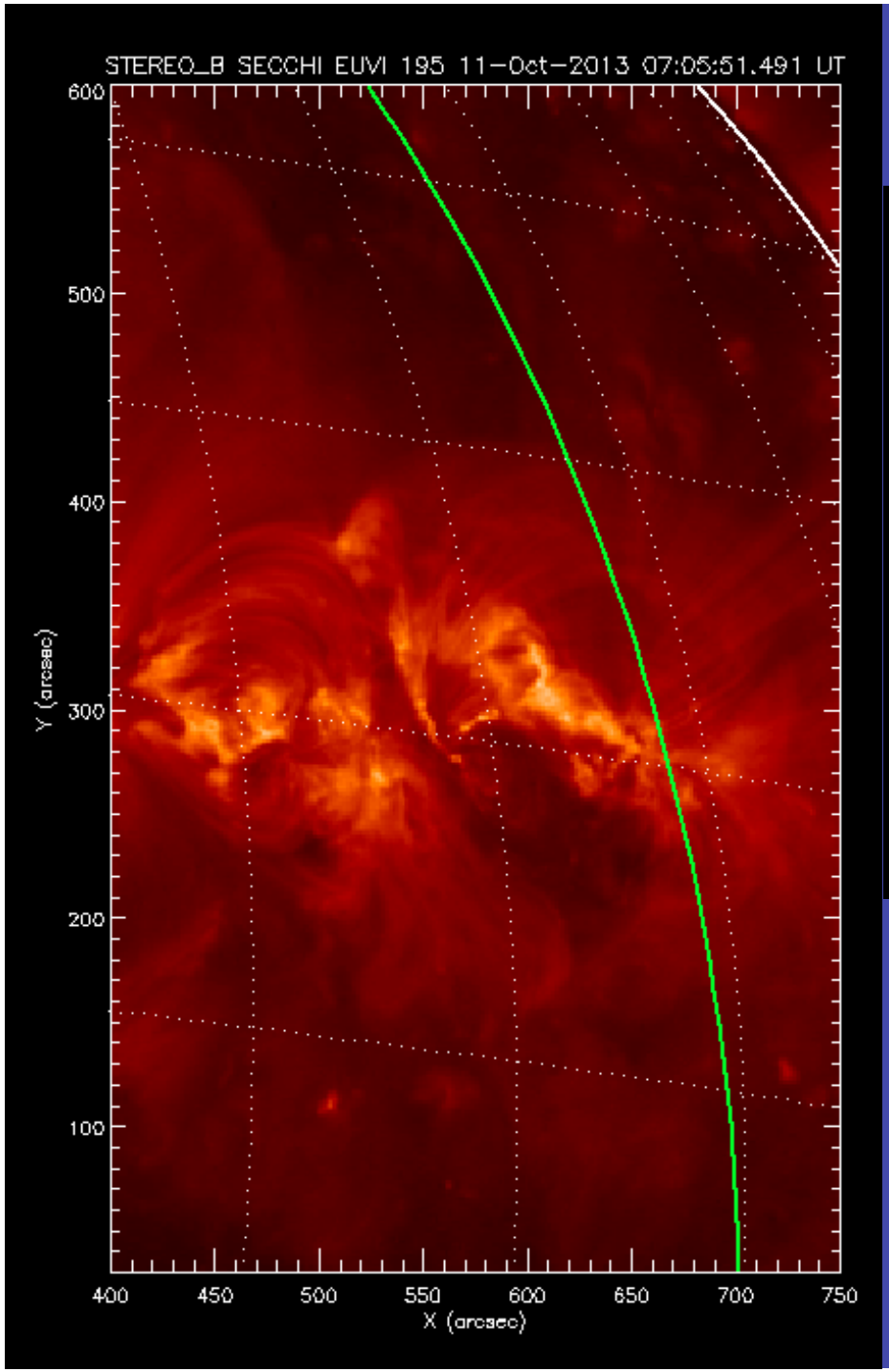

STEREO-Behind

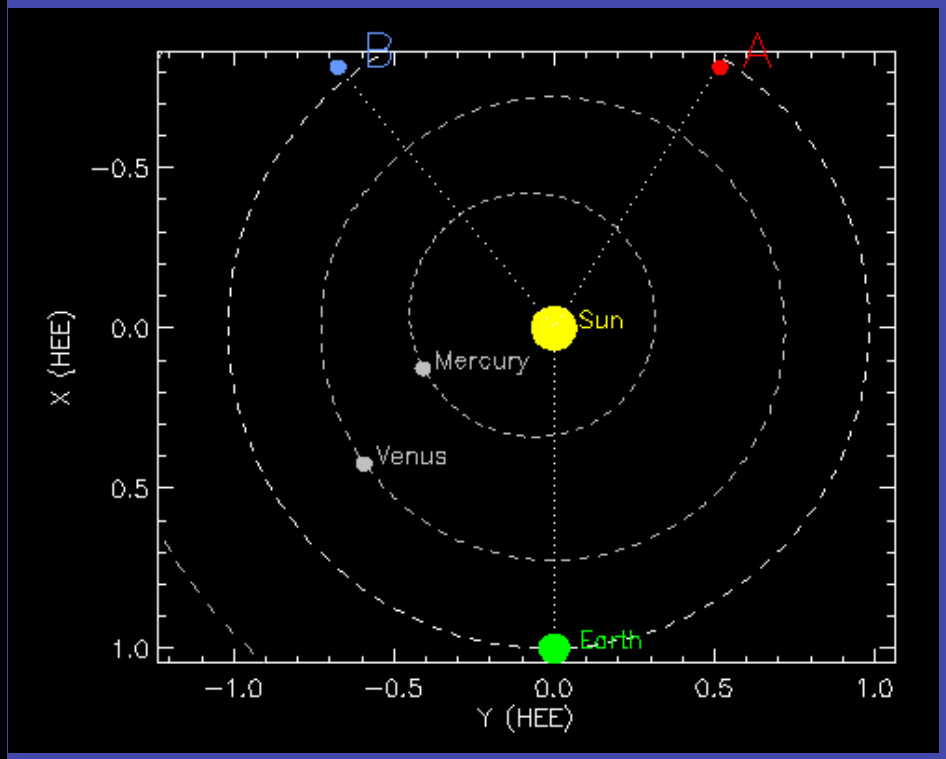

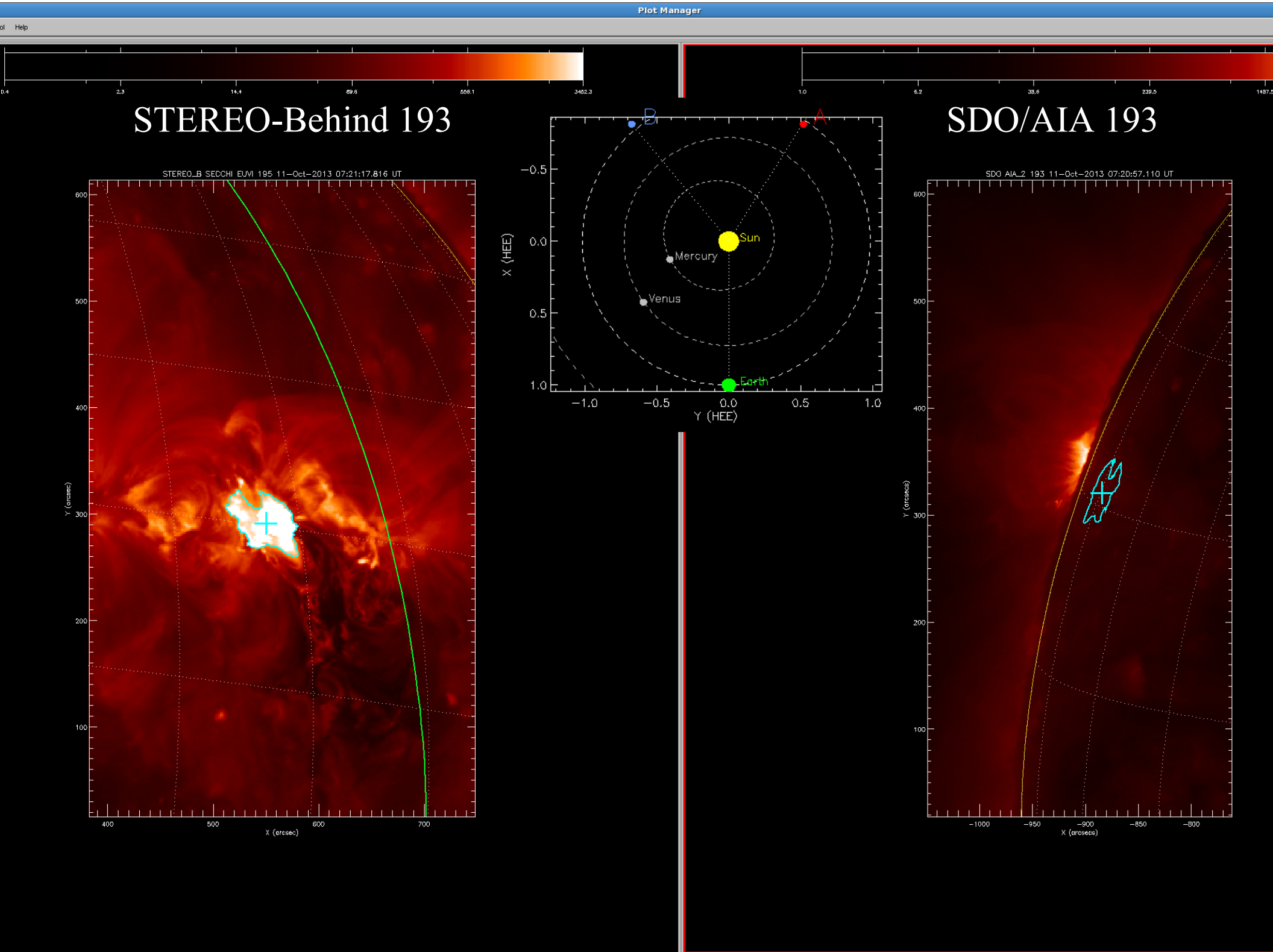
Plot Manager
STEREO-Behind 193
SDO/AIA 193
STEREO_B SECCHI EUVI 195 11-Oct-2013 07:21:17.816 UT
SDO AIA_2 193 11-Oct-2013 07:20:57.110 UT
X (arcsec)
Y (arcsec)
X (arcsecs)
Y (arcsecs)
X (HEE)
Y (HEE)
Sun
Mercury
Venus
Earth
A
B

RHESSI X-ray contours on SDO/AIA EUV images: coronal source only, footpoints occulted

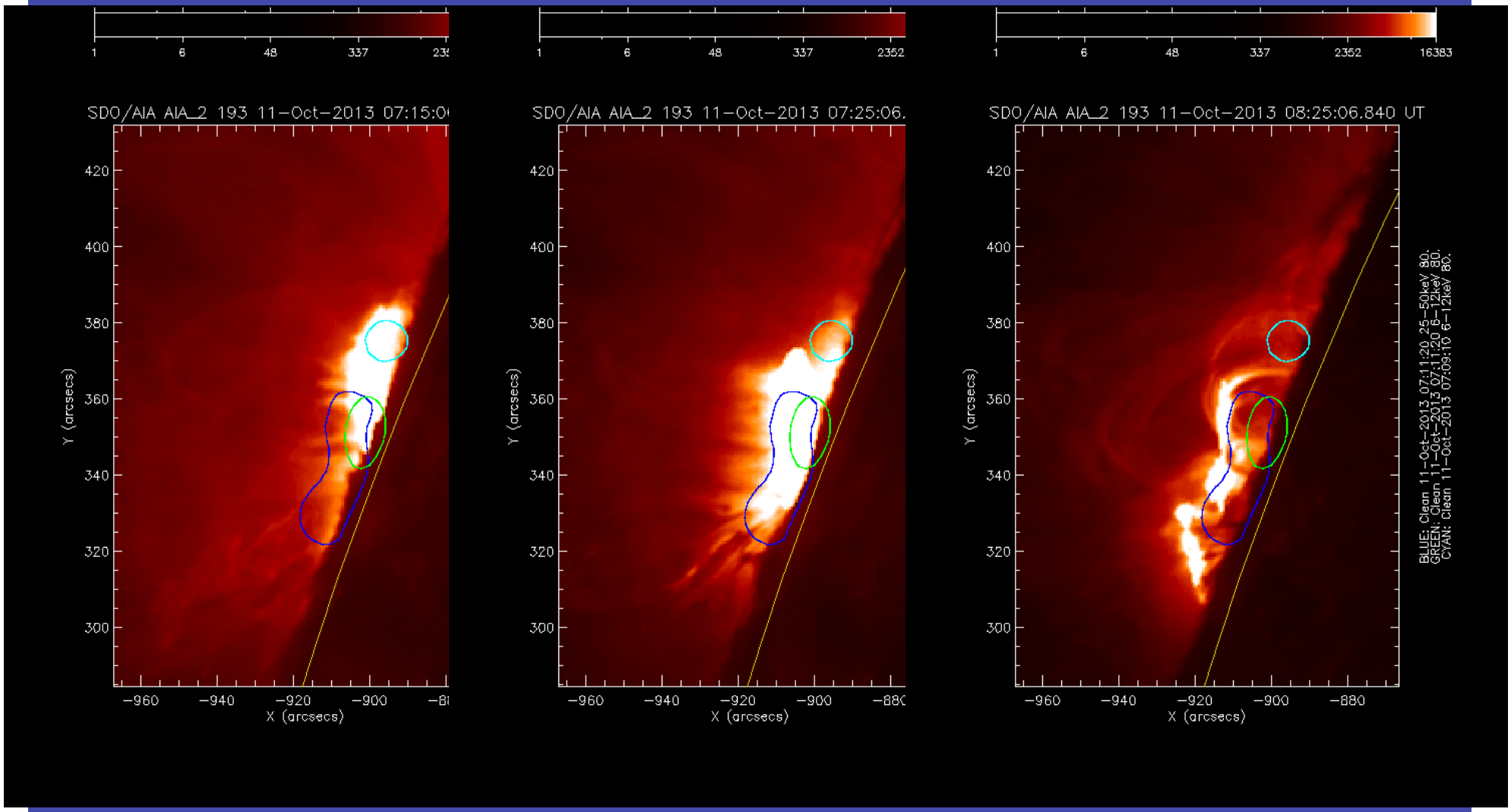

History of RHESSI X-ray source centroid height

Higher energy emission originates from greater heights => coronal (loop-top) source, rather than footpoint source => footpoints are occulted by the limb

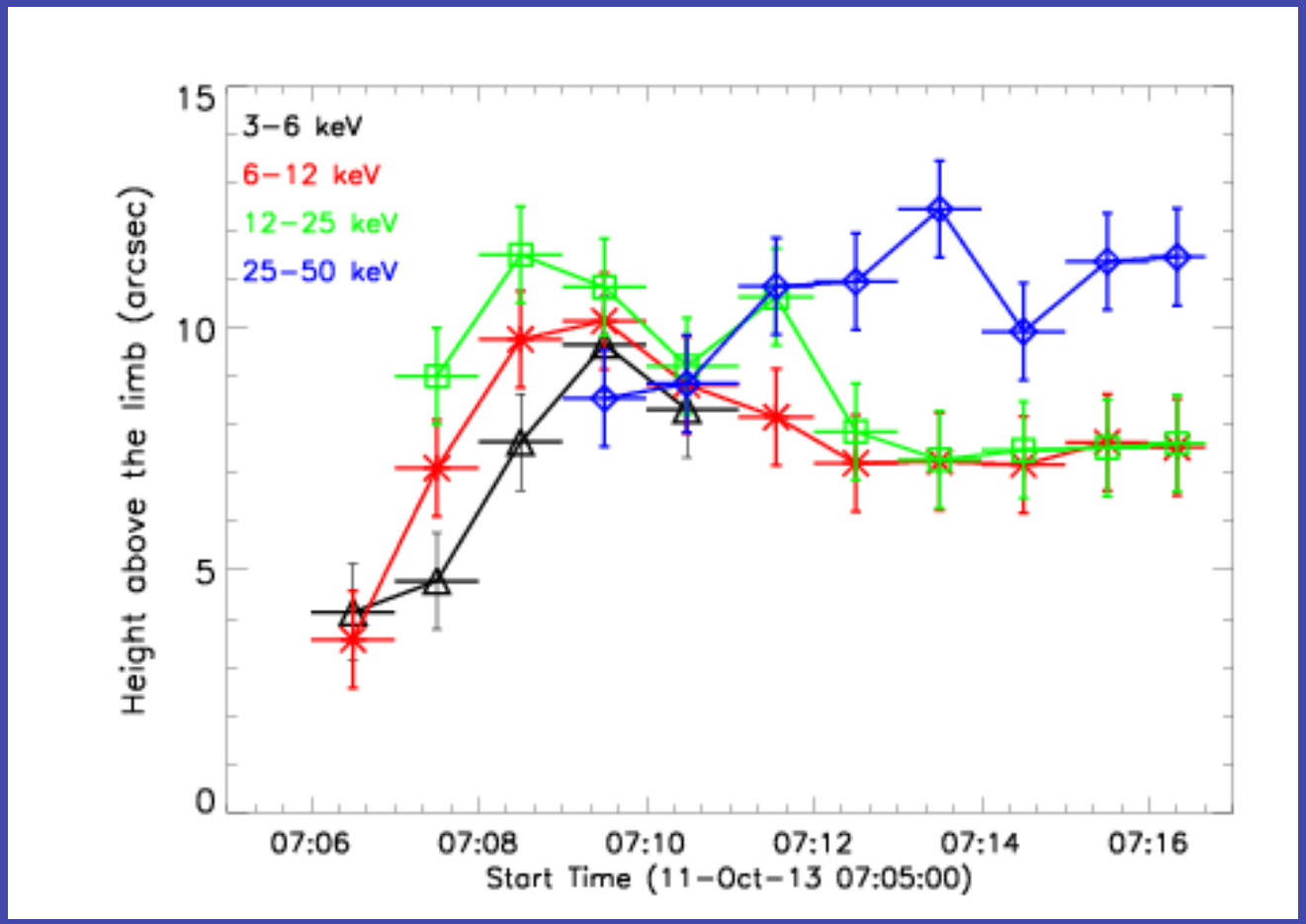

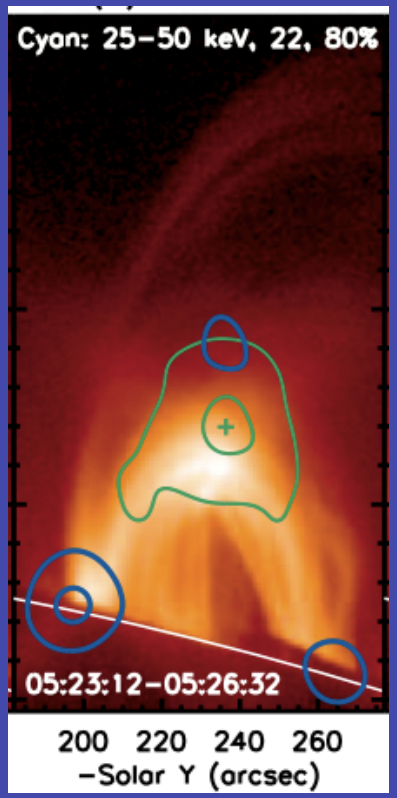

(Liu et al. 2013)

Fermi and RHESSI spectra

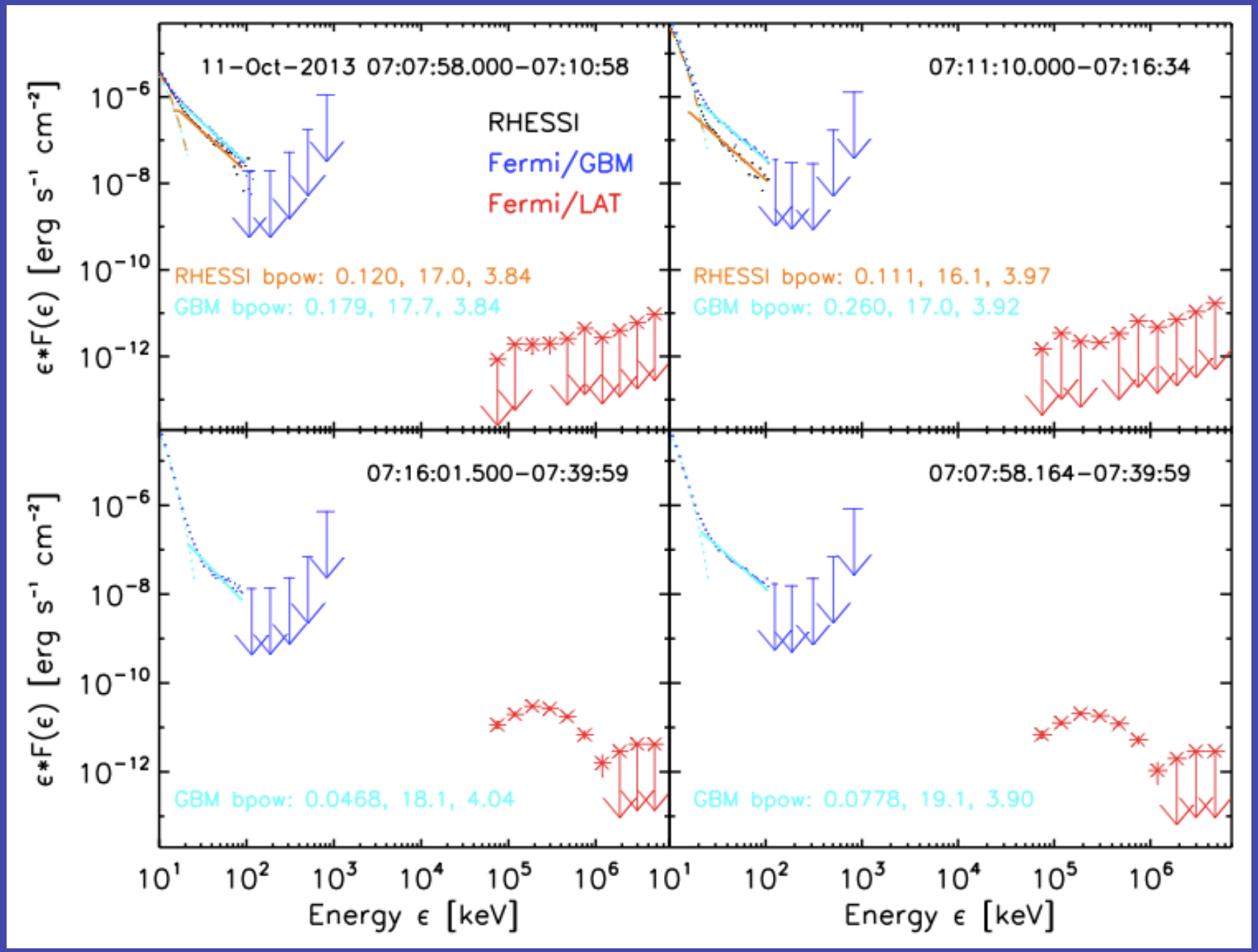

EUV wave (shock?) refraction from a remote active region

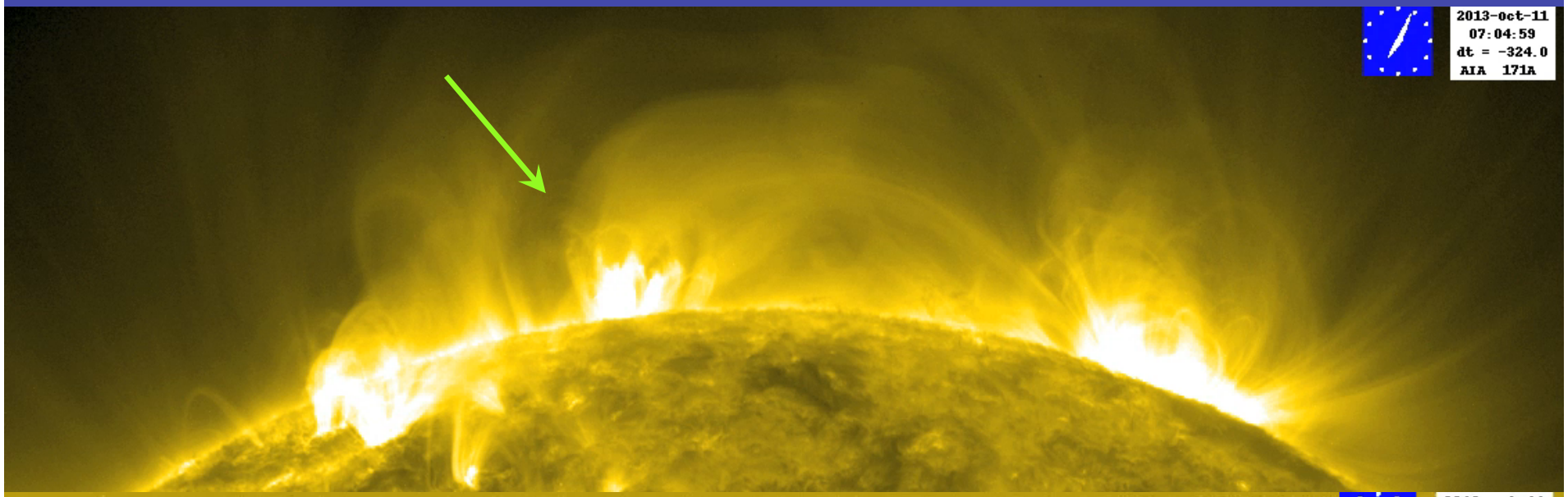

STEREO-B EUVI 195 Å

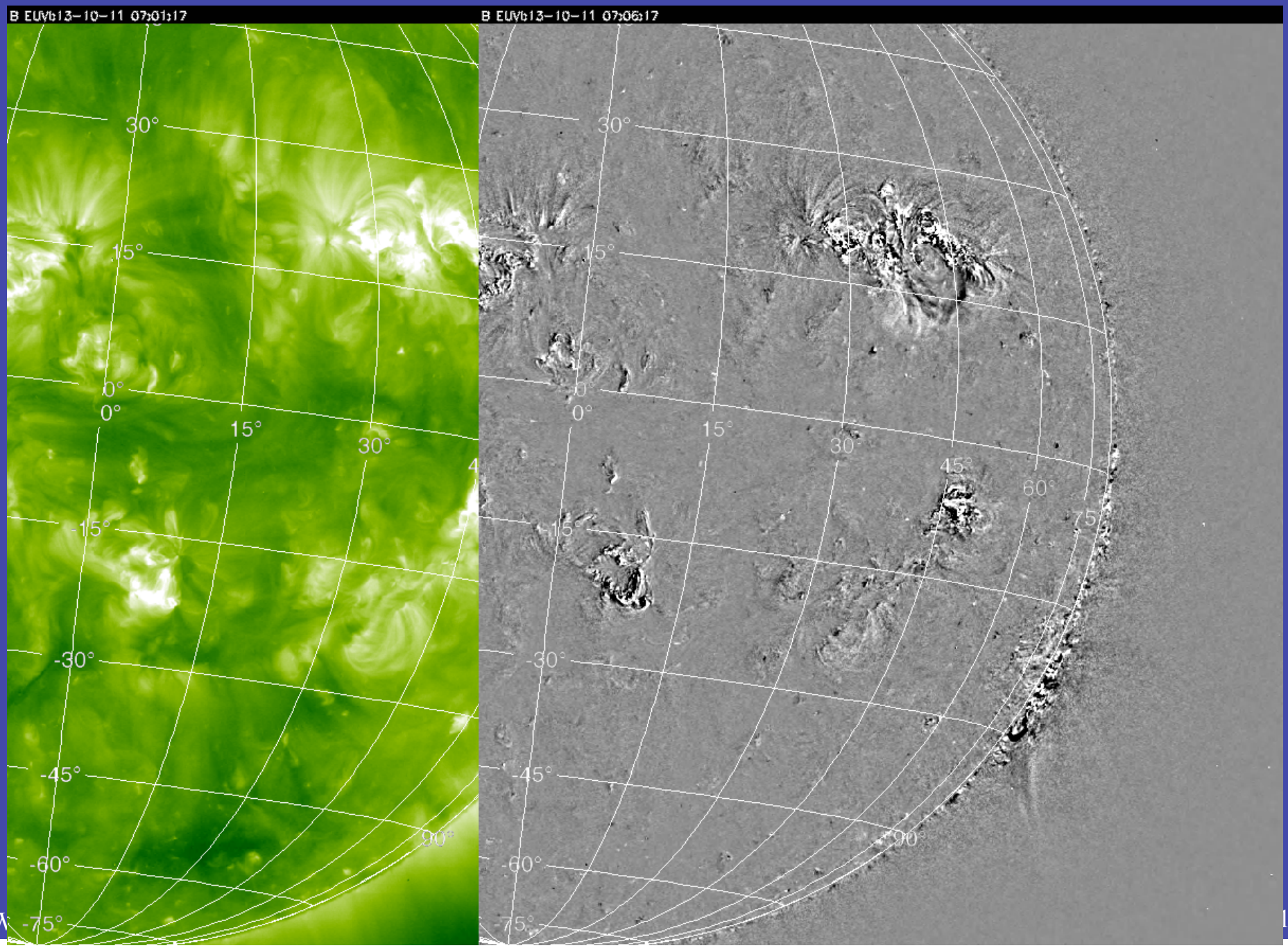

STEREO Radio type II bursts – CME driven shock

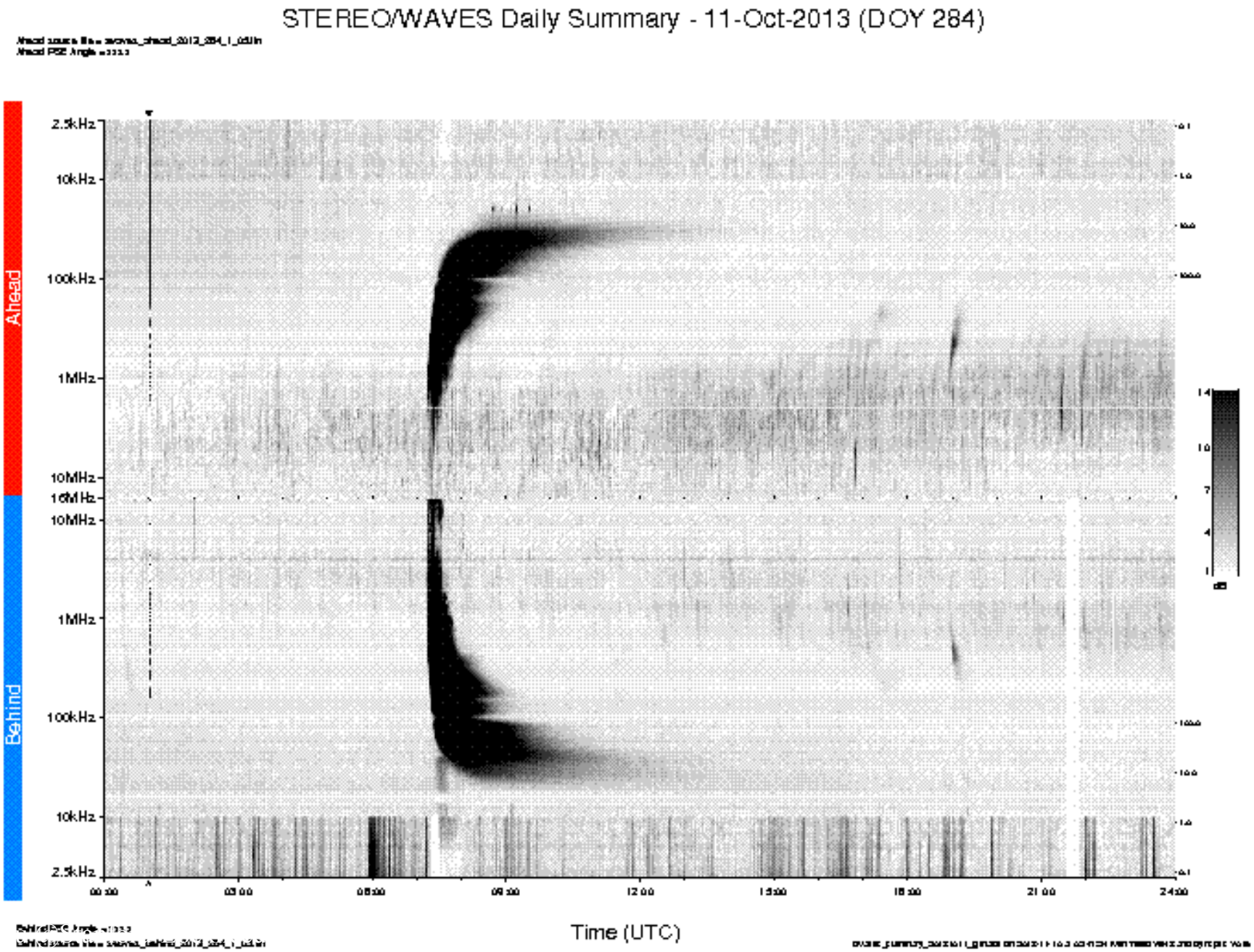

STEREO SEPs

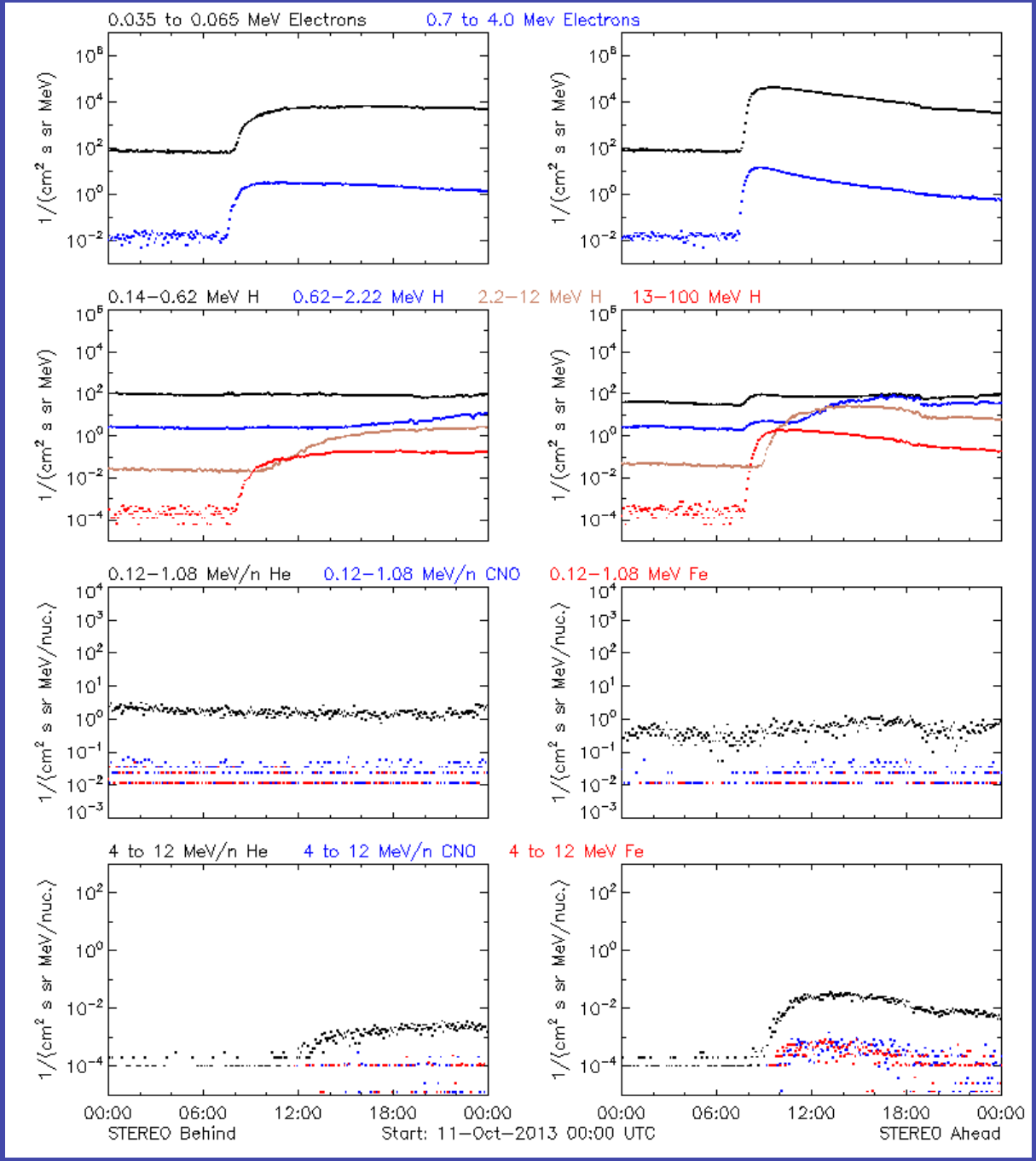
0.035 to 0.065 MeV Electrons
0.7 to 4.0 Mev Electrons
0.14−0.62 MeV H
0.62−2.22 MeV H
2.2−12 MeV H
13−100 MeV H
0.12−1.08 MeV/n He
0.12−1.08 MeV/n CNO
0.12−1.08 MeV Fe
4 to 12 MeV/n He
4 to 12 MeV/n CNO
4 to 12 MeV Fe
1/(cm² s sr MeV)
1/(cm² s sr MeV/nuc.)
00:00
06:00
12:00
18:00
00:00
STEREO Behind
Start: 11−Oct−2013 00:00 UTC
STEREO Ahead

Particle acceleration by shocks on the CME flanks traveling to the visible side of the solar disk?

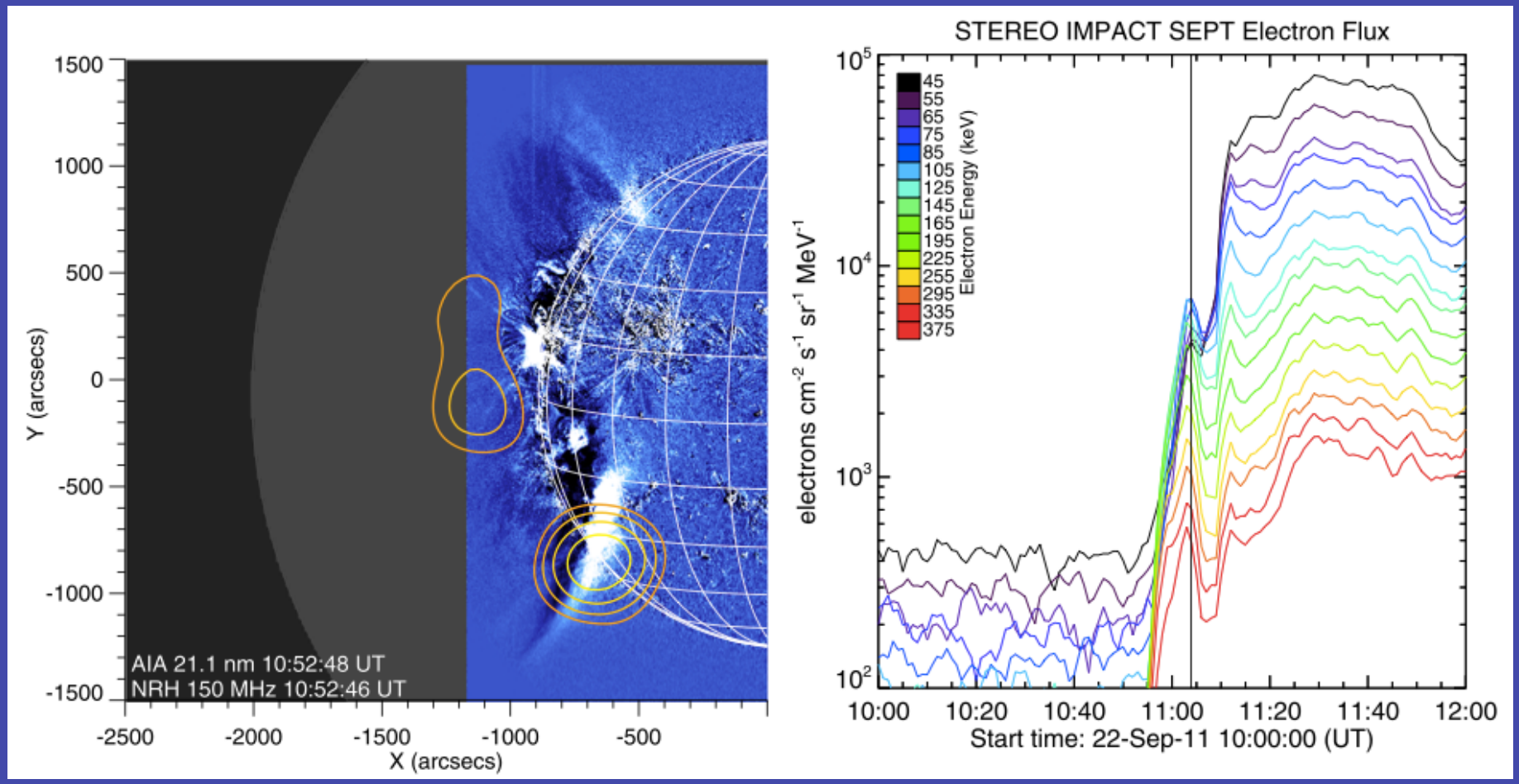

Carley et al. (2013)

3. Summary and Discussion

1) M1.5 Flare 11 degree behind East limb

2) Fermi/LAT detected γ-rays for ~30 minutes with energies up to 3 GeV

3) Three possibilities for the origin of γ-rays:

3.1) γ-rays penetrate solar interior at the limb at grazing angle – impossible for occultation angle > 2 deg

3.2) trapping of particles by magnetic mirroring, strong magnetic convergence and 1×10^{11} cm^{-3} density – still possible.

3.3) CME shock accelerated particles travel to the front side to produce γ-rays – possible

The End – Thank you

Backup slides:
New 2014/11/06

2. 2013-Oct-11 M1.5 flare, Fast (1200 km/s) CME seen by SOHO/LASCO

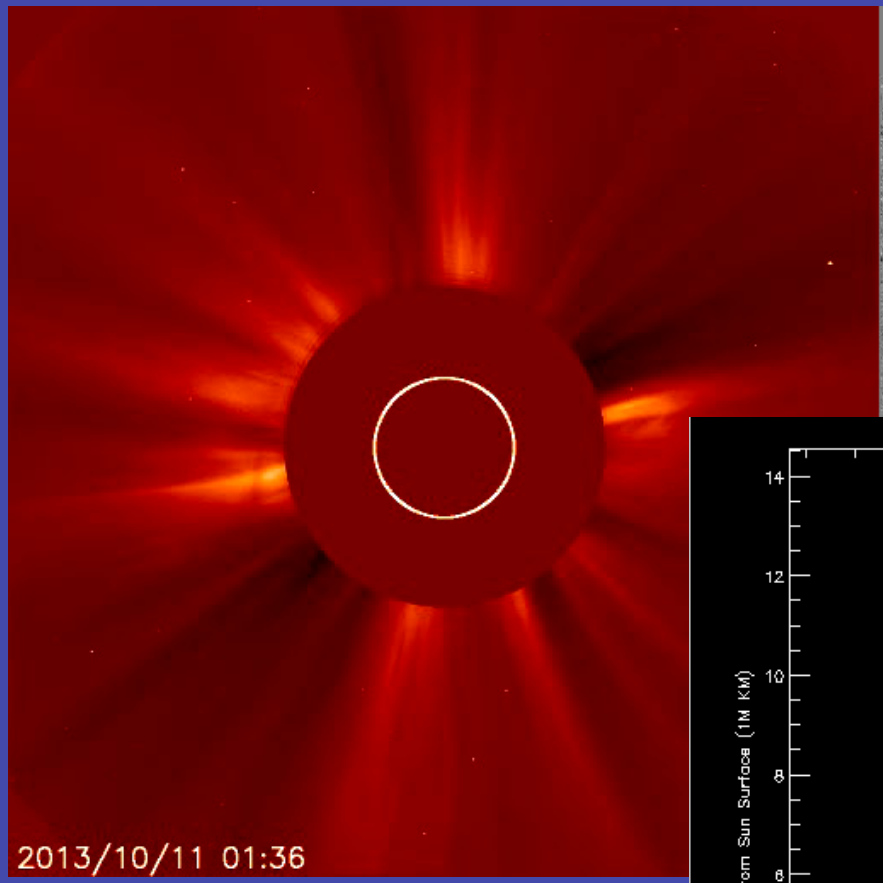

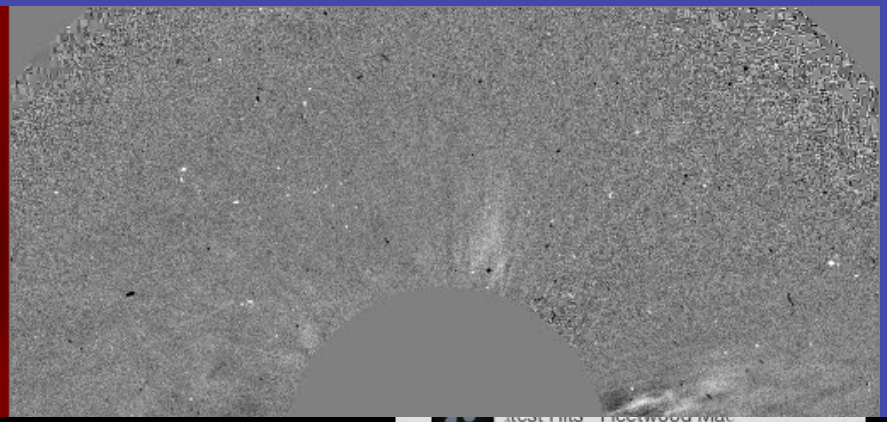

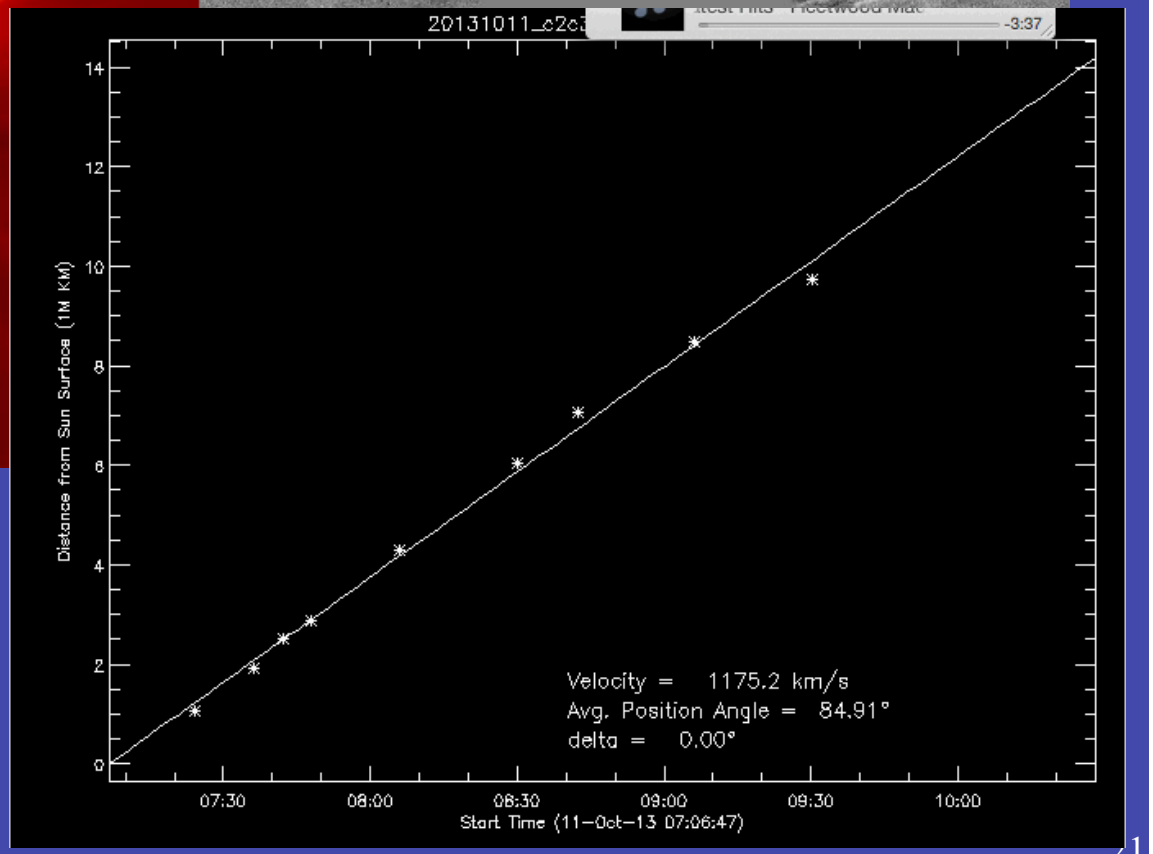

Gamma-ray absorption cross-section vs. photon energy

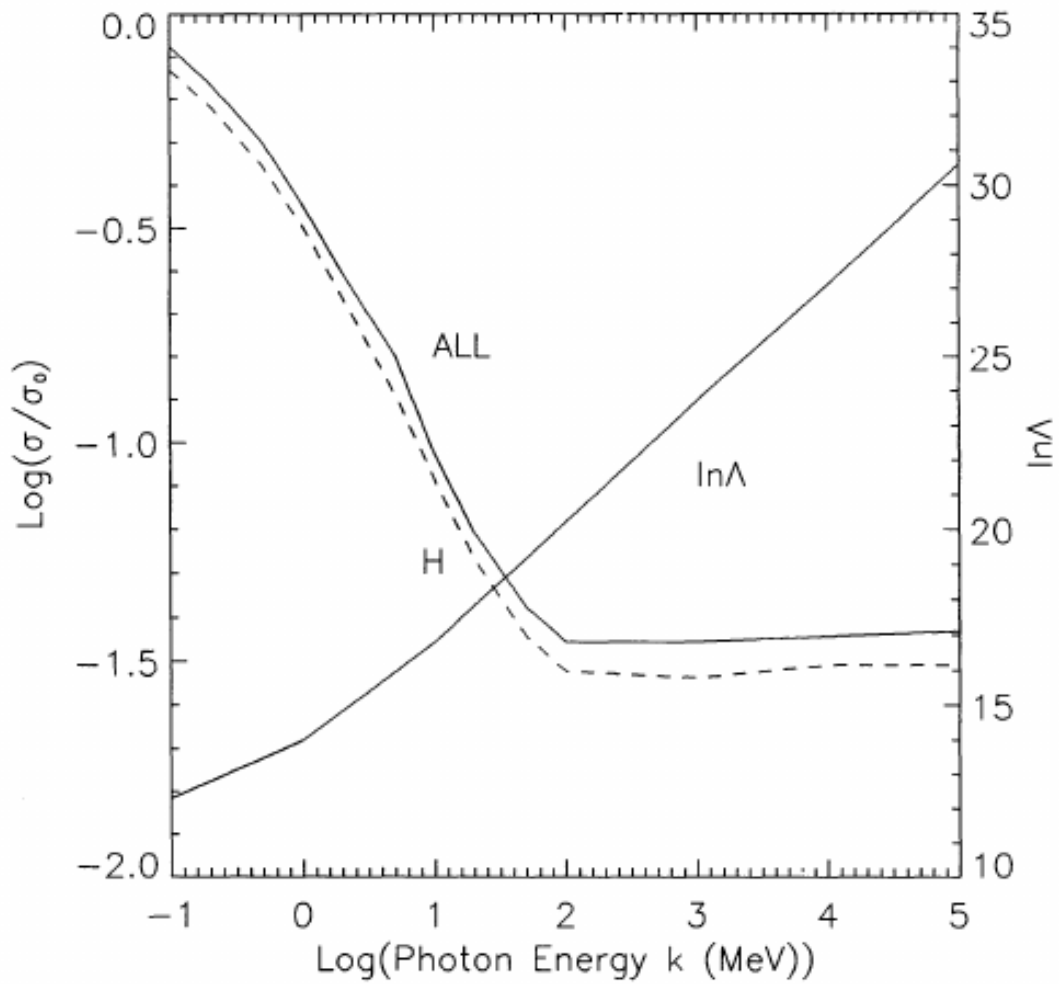

FIG. 5.—Variation with photon energy of the Coulomb logarithm ln Λ and total cross section (in units of Thompson cross section σ_0), primarily due to Compton scattering at low energies and pair production at high energies. The dashed line shows the cross section for hydrogen, and the solid line includes contribution of He and heavy elements for solar abundances calculated from compilation of cross sections by Hubbel et al. (1980).

From Petrosian (1994)

Fermi and RHESSI spectra fits

TABLE 2
SPECTRAL ANALYSIS OF LAT, GBM AND *RHESSI* DATA

LAT time intervals

Time Interval (2013/10/11 UT)	TS_{PL}	ΔTS^a	Γ	ϵ_{co}^b (MeV)	Flux^c 10^{-5} ph cm^{-2} s^{-1}	Proton index
07:10:00 – 07:15:00	16	5	$-1.8\pm0.3^{+0.007\,d}_{-0.003}$	–	$0.6\pm0.6^{+0.05}_{-0.04}$	–
07:15:00 – 07:20:00	987	22	$-0.2\pm0.3^{+0.007}_{-0.007}$	$145\pm27^{+0.72}_{-0.60}$	$24.1\pm1.5^{+1.59}_{-1.43}$	3.7 ± 0.2
07:20:00 – 07:25:00	1146	92	$-0.2\pm0.3^{+0.006}_{-0.003}$	$162\pm26^{+0.84}_{-0.31}$	$28.3\pm1.7^{+1.69}_{-1.51}$	3.5 ± 0.2
07:25:00 – 07:30:00	435	45	$0.4\pm0.6^{+0.007}_{-0.018}$	$96\pm22^{+0.33}_{-0.76}$	$13.7\pm1.3^{+0.84}_{-0.75}$	4.3 ± 0.4
07:30:00 – 07:35:00	55	4	$-2.4\pm0.2^{+0.002\,d}_{-0.002}$	–	$4.1\pm4.1^{+0.37}_{-0.32}$	–

RHESSI and GBM time intervals

	Cutoff energy (keV)	Power-law index	Flux ph cm^{-2} s^{-1}	Plasma temperature KT (keV)
07:08:00 – 07:10:58*	17.00	3.84	2.99	2.19
07:08:00 – 07:10:58	17.73	3.84	3.42	2.49
07:11:10 – 07:16:40*	16.09	3.97	2.77	1.99
07:11:10 – 07:16:40	17.01	3.92	4.11	2.27
07:16:40 – 07:35:00	18.10	4.04	1.75	1.89
07:08:00 – 07:35:00	19.14	3.92	1.94	1.82

History of wave fronts ➔ wave paths ➔ map of fast-mode speeds ➔ map of magnetic field strengths

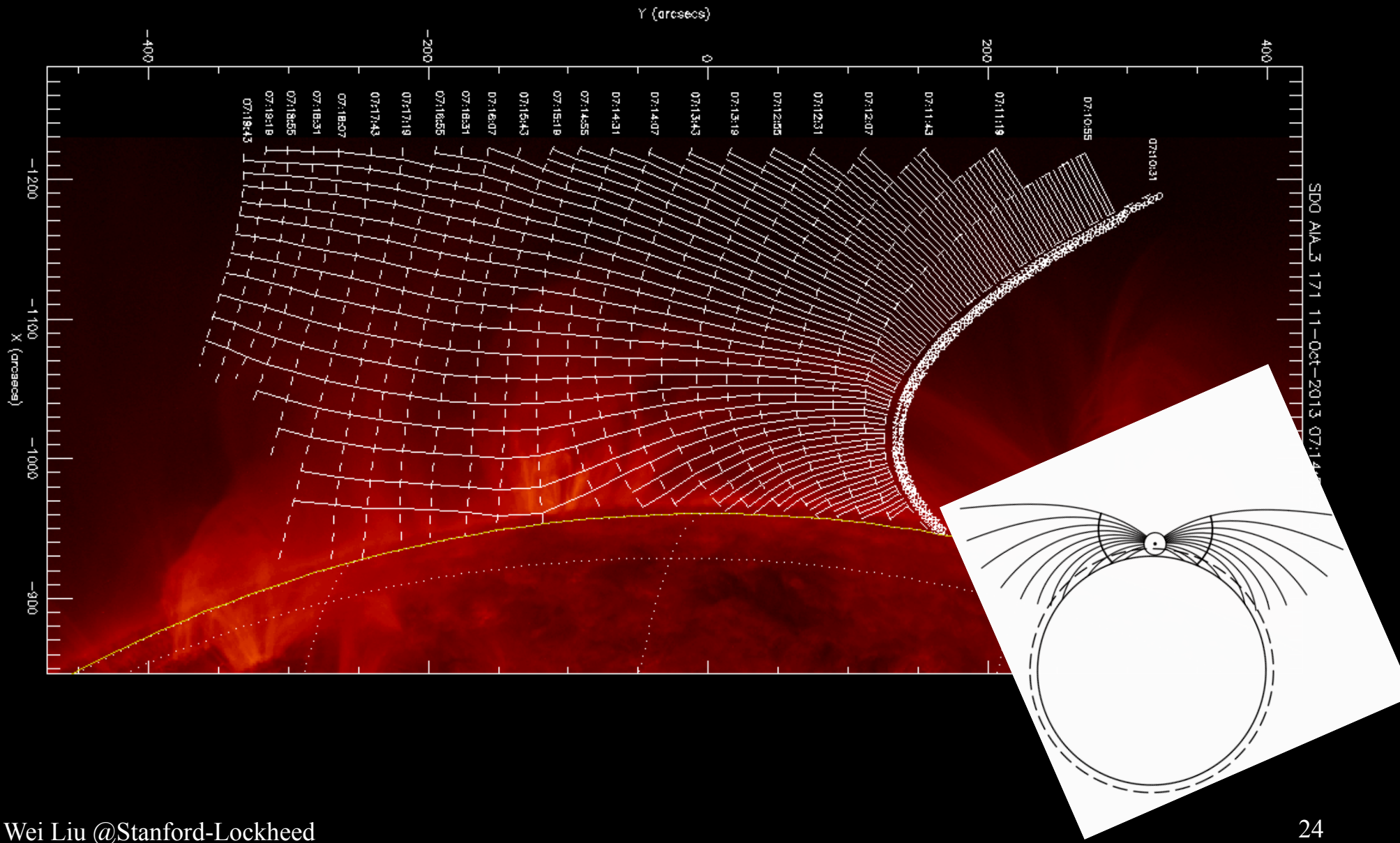

The End – Thank you